THEORETICAL STUDY OF BIPOLARON DYNAMICS IN POLYPARAPHENYLENE: II. DENSITY FUNCTIONAL THEORY (DFT) CALCULATIONS ON NEUTRAL DIMERS AND SEMIEMPIRICAL HÜCKEL-TYPE CALCULATIONS ON NEUTRAL AND CHARGED MODEL CHAINS

Wolfgang FÖRNER

Department of Chemistry, King Fahd University of Petroleum and Minerals, Dhahran 31261, Saudi Arabia; e-mail: forner@kfupm.edu.sa

Received October 26, 2004
Accepted March 29, 2005

Dedicated to Professor Josef Paldus on the occasion of his 70th birthday

We have derived earlier the rather lengthy formalism for time simulations in poly(*p*-phenylene), treating the rings as semirigid rotors. To this end the Euler–Lagrange formalism had to be used. As a first step we intended to parametrize the simplified Hückel-type hamiltonian on the basis of density functional theory (DFT) calculations on some dimeric model systems. The results of this attempt are reported here. However, calculations on much longer chains, containing up to 200 rings, show a clear tendency of our model to favor the quinoid B-phase structure over the aromatic one. Further, in doubly charged chains, the charge tends to remain unseparated and to be completely delocalized over virtually the complete part of the chain, that is in B-phase conformation. The bipolaron width turns out to be extremely small, of about 10 rings in a chain having 200 rings. This is rather unexpected and interpreted as a shortcoming of the Hückel-type nature of the hamiltonian. The reason is that in the Hückel-type model the two electrons, taken away to charge the chain, are from the same orbital, and thus charge separation is more difficult, leading, in this case, only to a delocalization, keeping the bipolaron small. We assume, that in line with Prof. Paldus' work, the inclusion of direct electron–electron interactions in the form of a Pariser–Parr–Pople (PPP) type model could overcome this difficulty. The treatment has to be done, probably, in an open shell form to make possible spin separation, if necessary. Care has to be taken for spin contaminations in such treatments and possibly even the explicit inclusion of electron correlation might be necessary. In this paper we report our model which was derived in detail in a previous paper. Then we discuss the parametrization attempts and our results on longer chains. In conclusion our suggestion is that a PPP type model must be used at least to allow for bipolaron calculations and confinement of the two like charges. Such calculations would be the content of a forthcoming paper.

Keywords: Poly(*p*-phenylene); DFT calculations; Parametrization of a Hückel-type model; Static model calculations; *Ab initio* calculations; Pariser–Parr–Pople model.

I. INTRODUCTION

Conjugated organic polymers like *trans*-polyacetylene (tPA) or poly(*p*-phenylene) (PP), usually exhibit spinless charge transport at low doping levels. In tPA this phenomenon was explained initially and successfully by Su, Schrieffer and Heeger (SSH) with the help of solitons[1–4]. tPA shows a dimerized structure in the ground state, i.e. longer "single bonds" and shorter "double bonds" alternate. Obviously this leads to the existence of two energetically degenerate ground states with different bond alternation phases (termed A and B). If in a given chain we have a defect where this phase passes from A to B we have a soliton. Such a soliton can be electrically charged (spinless) or neutral (see[1–3], a detailed review paper, authored by KSSH, K denoting Kivelson, is cited as[4]). The charged solitons are then the charge carriers in the observed charge transport without the transport of spins in tPA at low doping levels or in the photoconducting state. Already in their first simulations of the dynamics of tPA with the help of the Su–Schrieffer–Heeger model[1–3], Su and Schrieffer[5] have found that, upon doping of soliton-free tPA chains with one electron or hole, no solitons but charged polarons are formed. These polarons are defects, which can be viewed as a bound state of a soliton (phase change from A to B) and an anti-soliton (phase change from B to A), where one of them is charged. However, one could show that bipolarons, i.e. doubly charged polarons, are instable in tPA because of the degenerate ground state and they decay rapidly into a pair of free charged solitons[4–6]. But, as discussed below, in polymers like poly(*p*-phenylene), bipolarons (doubly charged and spinless) can be stable, while solitons are not. We want to point out that the findings of SSH at most were obtained with a simple Hückel-type hamiltonian which in contrast to the Hückel model incorporates variations of the resonance integrals with bond lengths.

Further it has been shown that the SSH model, which is basically of a Hückel type without any explicit electron–electron (e–e) interaction included, is not sufficient to describe tPA. We do not intend to list here all the arguments for the importance of e–e interactions in conducting polymers, but refer the reader to the detailed discussion given by Baeriswyl[7]. We have studied the dynamics of polarons and bipolarons in tPA, including e–e interactions on the Pariser–Parr–Pople[8–12] (PPP) level[13,14]. We have found that e–e interactions considerably reduce the extension of solitons in tPA chains (present there at very low doping levels). Bipolarons are unstable on the PPP level and decay into free, charged solitons within a very short time, leaving a breather vibration behind them. Similar results were obtained by

Boudreaux et al.[15] with the help of the semiempirical all-valence electron MNDO (modified neglect of differential overlap) method, which includes, in contrast to the PPP model, not only the π electrons, but all the valence electrons. Our studies on PP will be based on our experience gained in the work on tPA and cPA (*cis*-PA). However, due to the success of the Hückel-type SSH model in simple polyacetylene chains we want to report in this paper the shortcomings of Hückel-type models when applied to more complicated systems like PP. As detailed in Conclusion, we suggest that the shortcomings are really due to the lack of explicit electron–electron interactions and advocate, like Prof. Paldus did many times, the use of at least a PPP approach for such systems.

On the basis of theoretical considerations it has been concluded that the coupling between different chains (although weak) should destabilize polarons[16,17]. Also the results of three-dimensional density functional band structure calculations seem to point to this direction[18]. More recent work, however, indicated that short chain lengths as well as impurities are able to stabilize polarons[19]. Also, investigations using the SSH model have shown that polarons can be stable within a broad range of the coupling strength between different chains[20]. Further, polarons were observed experimentally[21,22]. With the help of the valence effective hamiltonian (VEH) method it was possible to calculate the number and the energetical positions of the electronic excitations due to a polaron, in agreement with experimental data[23]. The influence of quantum lattice fluctuations on the dimerization and on solitons in tPA was investigated using different methods[24–28]. The mobility of solitons and polarons in the presence of the effects of scattering on acoustic lattice phonons was investigated by Sum et al.[29], where a surprisingly large difference in mobility between charged and neutral quasiparticles was found.

In *cis*-PA (cPA) as well as in most of the other conducting organic polymers like PP, two states also exist with different bond alternation phases. However, in contrast to tPA, in these systems the two states are not energetically degenerate. This implies that solitons cannot be stable in this type of material[3] because they represent a change from A to B form at the soliton center and therefore would be associated with a large chain segment of high energy B phase. Thus they would simply move to the chain end and remain there forever, or they would deform the chain around them to a polaron (singly charged, not spinless), which contains limited amount of B phase only. Separating pairs of charged solitons would develop a chain segment of increasing length between their centers which would show the energetically unfavourable B phase. Therefore polarons could exist in these

systems, and also bipolarons, because the electrostatic repulsion between the two charges of a bipolaron could be compensated via the small B-segment in a bipolaron in contrast to the very long one which would be necessary for complete separation of the charges. The stability and dynamics of such polarons have been investigated theoretically, although mostly on the SSH level[20,30]. The static properties of such quasiparticles have also been studied using all-valence electron methods[31–34]. Investigations of the influence of e–e interactions on polarons and bipolarons in cPA have been studied by us and also by other groups.

However, most of the other synthetic metals do not have a degenerate ground state, just like cPa, and therefore support polarons and bipolarons as charge carriers. An important polymer of this type is poly(*p*-phenylene). PP and other polymers of this type are blue-light-emitting, and therefore are potential candidates for light emitting diodes. Our main interest are time simulations on the charge carriers in this material. To that end, we have to reparametrize the SSH-type hamiltonian on the basis of *ab initio* calculations on some dimers of the monomer of PP (biphenyl), after having derived the formalism needed for the model in Section II. The formalism for the time simulation, based on the Euler–Lagrange approach was derived and outlined in previous papers[35,36]. Since, due to the shortcomings of the single-particle model, we actually do not report any simulations in this paper, we will only discuss the model geometry, the σ electron potential and the π-electron energy in Section II.

In a forthcoming paper which is presently under investigation we hope that we can report on the parametrization of a PPP hamiltonian as well as on bipolaron optimizations and time simulations. Further we plan to study electronic spectra of the doped polymer.

II. METHOD

As mentioned earlier, in this Section we want to outline first of all our geometrical model and the collective coordinates, governing the movements. This model is based on optimized structures of biphenyl and terphenyl, using the density functional theory (DFT) method. In Subsection 2 we want to present our Hückel-type model for the π-electrons. Finally, in Subsection 3 the potentials which could model the σ-electrons are outlined. Since in Section III we want to report some results, pointing to the shortcomings of such a model, there is no need to detail here the time simulation method, which was already published[36].

II.1. Geometry

As reported in our previous papers[35,36], we initially wanted to build a complete chain from repetition of the central unit of terphenyl, rotated $(J-1)$ times by the equilibrium rotation angle ($\varphi_o^A = 38.4°$ in biphenyl, $\varphi_o^A = 37.9°$ in terphenyl) for the ring number J, the first ring and the reference geometry being in the *xy*-plane as indicated in Fig. 1. This rotation pattern could be simulated by a linear extrapolation between the angles for the aromatic and the quinoid form, according to the aromatization coordinate q_J of ring J and that of its $(J-1)$-th neighbor.

The atomic coordinates, $\boldsymbol{R}'_{Ji}$, of a ring in the same position as the reference ring, being in an aromatic geometry ($\boldsymbol{R}_i$) can be generated by (following[36])

$$\boldsymbol{R}'_{Ji} = \boldsymbol{R}_i + \frac{1}{2}(1\text{Å} - q_J)\,\boldsymbol{\Delta}_i \,. \qquad (1)$$

Note, that the terminal rings, besides being in the *xy*-plane, do not necessarily need to have the reference geometry. The shift vectors together with the reference ones and the necessary parameters are given in Table I. The translation t has to be performed $(J-1)$ times along x to shift the ring into position J.

While in[36] we suggested to use the geometry of the central unit in terphenyl as reference for all the units of a chain, the DFT potential surfaces for dimeric structures, published in[35], suggest that the geometrical model should be more close to reality. So we decided to use for the dimer directly the biphenyl geometry, while chains with a larger than or equal to

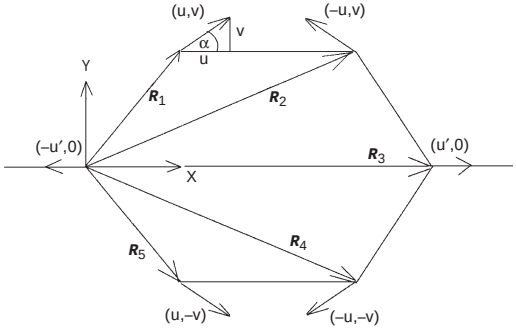

FIG. 1
Sketch of the structural parameters in the central unit of terphenyl and the B-phase trimer

TABLE I

The reference geometries R^j, where j denotes the ring involved (atom #6 is always shifted to the origin) and the shift vectors $\boldsymbol{\Delta}^j$, connecting the aromatic form to the quinoid one in the dimers and the trimers of poly(*p*-phenylene) (calculated by the DFT/B3LYP method). Note that all the rings are planar and thus all *z*-coordinates are equal to zero. Only by rotations of individual rings by Φ around *x* do they come into play. The angles given are for the purely aromatic forms and *t* is the length of the translation vector along *x* leading from one ring to the next one on its right hand side. *j* here is 1 or *N* (2 for the dimer) for the two terminal units and *i* for all rings inside the chain

Dimer (Φ = 38.3850°)

Left terminal unit	$\boldsymbol{R}^1$, Å		$\boldsymbol{\Delta}^1$	
Atom	*x*	*y*	*x*	*y*
1	0.703665	1.205427	u	v
2	2.097527	1.205099	–u′	v′
3	2.820094	0.0	w	0
4	2.097527	–1.205099	–u′	–v′
5	0.703665	–1.205427	u	–v
6	0.0	0.0	–w	0

u = 0.0274700 Å, *v* = 0.0220242 Å, *u′* = 0.0101100 Å, *v′* = 0.0179049 Å, *w* = 0.0457660 Å, *t* = 4.3059640 Å

Right terminal unit	$\boldsymbol{R}^2$, Å		$\boldsymbol{\Delta}^2$	
Atom	*x*	*y*	*x*	*y*
1	0.722567	1.205099	u′	v′
2	2.116429	1.205427	–u	v
3	2.820094	0.0	w	0
4	2.116429	–1.205427	–u	–v
5	0.722567	–1.205099	u′	–v′
6	0.0	0.0	–w	0

TABLE I
(*Continued*)

Trimer (Φ = 37.9143°)

Left terminal unit	$\boldsymbol{R}^1$, Å		$\boldsymbol{\Delta}^1$	
Atom	*x*	*y*	*x*	*y*
1	0.703677	1.205464	u_1	v_1
2	2.097436	1.205283	$-u_1'$	v_1'
3	2.820166	0.0	w_1	0
4	2.097436	–1.205283	$-u_1'$	$-v_1'$
5	0.703677	–1.205464	u_1	$-v_1$
6	0.0	0.0	$-w_1$	0

u_1 = 0.0281975 Å, v_1 = 0.0199442 Å, u_1' = 5.368500 × 10^{-3} Å, v_1' = 0.0137843 Å, w_1 = 0.0425795 Å, t = 4.3045150 Å

Central unit	$\boldsymbol{R}^i$, Å		$\boldsymbol{\Delta}^i$	
Atom	*x*	*y*	*x*	*y*
1	0.728267	1.201195	u	v
2	2.119443	1.201195	–u	v
3	2.847710	0.0	w	0
4	2.119443	–1.201195	–u	–v
5	0.728267	–1.201195	u	–v
6	0.0	0.0	–w	0

u = 0.0121170 Å, v = 6.878000 × 10^{-3} Å, w = 0.0350050 Å

Right terminal unit	$\boldsymbol{R}^N$, Å		$\boldsymbol{\Delta}^N$	
Atom	*x*	*y*	*x*	*y*
1	0.722730	1.205283	u_1'	v_1'
2	2.116489	1.205464	$-u_1$	v_1
3	2.820176	0.0	w_1	0
4	2.116489	–1.205464	$-u_1$	$-v_1$
5	0.722730	–1.205283	u_1'	$-v_1'$
6	0.0	0.0	$-w_1$	0

$N = 3$ number of rings, have the terminal units of terphenyl at their ends and all rings aside from the terminal ones have the central unit of terphenyl (see Table I). The shifts are now taken directly from the atomic coordinates and not as previously suggested from the changes in bond lengths between A and B phases.

Then the aromatization coordinates of the J-th and the $(J-1)$-th ring would determine the relative rotation angle between the two rings. In a first approximation one could assume that the mean value of the two q-s is mainly responsible for the actual value of the relative angle:

$$\varphi_J = \frac{1}{2}\left(\frac{1}{2}(q_J + q_{J-1}) / \text{Å} + 1\right) \phi_o^A \,. \tag{2}$$

Thus to obtain the positions $\boldsymbol{R}_{Ji}$ in ring J, the above, shifted geometry would have to be rotated around the x-axis by (note that $\varphi_1 = 0$)

$$\Phi_J = \sum_{I=2}^{J} \varphi_I \tag{3}$$

and then shifted $(J-1)$ times by the translation length t:

$$\boldsymbol{R}_{Ji} = \boldsymbol{D}_x(\Phi_J)[\boldsymbol{R}_i + \frac{1}{2}(1\text{Å} - q_J)\,\boldsymbol{\Delta}_i] + (J-1)\,t\boldsymbol{e}_x$$

$$\Phi_J = \frac{1}{2}\sum_{I=1}^{J}\left(1 - \frac{1}{2}\delta_{I1} - \frac{1}{2}\delta_{IJ}\right)\phi_o^A q_I / \text{Å} + (J-1)\frac{\phi_o^A}{2} \,. \tag{4}$$

$\boldsymbol{e}_x$ is the unit vector in x direction and the relevant values for t are given in Table I. The rotation matrix $\boldsymbol{D}_x(\alpha)$ is

$$\boldsymbol{D}_x(\alpha) = \begin{pmatrix} 1 & 0 & 0 \\ 0 & \cos\alpha & \sin\alpha \\ 0 & -\sin\alpha & \cos\alpha \end{pmatrix}. \tag{5}$$

However, note that in our finalized formalism, we allow the rotation angles at the rings to vary freely. Only the angle at ring #1 is always fixed to zero. Also any additional CH_2 groups for the saturation of dangling bonds in the quinoid forms are always attached in a coplanar structure to rings 1 and N. Their coordinates are:

$$R_{6N+1} = \left\{ x^0_6 - \left[r'_A + \frac{1}{2}(1\,\text{Å} - q_0)\,\Delta'_{AB} \right] \right\} \boldsymbol{e}_x$$

$$R_{6N+2} = \left\{ x^0_3 + \left[r'_A + \frac{1}{2}(1\,\text{Å} - q_{N+1})\,\Delta'_{AB} \right] + (N-1)t \right\} \boldsymbol{e}_x \,, \qquad (6)$$

where the $x^0{}_i$ are the x coordinates of the carbons #3 and #6 in the reference geometry, r'_A = 1.485870 Å, r'_B = 1.405162 Å in the dimer, r'_A = 1.484349 Å, r'_B = 1.406069 Å in all longer chains (numbers from the trimer), and $\Delta'_{AB} = r'_B - r'_A$. The values of t can be found in Table I, the q-values for these carbons are varied freely and their rotation angles are the same as those of the neighboring rings (1 and N, respectively). A ring in its unshifted and unrotated (around x) position is sketched in Fig. 1, which gives also the atom numbering in a ring.

II.2. The Hückel-type Model for the π-Electrons

II.2.1. The Model

For the calculation of the π-electron energy we use a semiempirical Hückel-type method in a similar manner as SSH did for tPA. We do not need to describe the method here in an open shell form, because for a Hückel-type picture the orbitals for α- and β-spin are the same, as well as their eigenvalues, only their occupation numbers differ in the case of open shells. The basic eigenvalue problem that has to be solved is

$$\boldsymbol{H}\boldsymbol{c}_i = \varepsilon_i \boldsymbol{c}_i \,. \qquad (7)$$

The overlap matrix, usually appearing in *ab initio* problems reduces here to the unit matrix, because of the zero differential overlap approximation (ZDO) applied in Hückel type models. The $\boldsymbol{c}$-s denote the column eigenvectors of the Hückel matrix $\boldsymbol{H}$, and the ε-s the energy eigenvalues. In Hückel type theories a p orbital is assumed at every carbon atom and the one electron wavefunctions are linear combinations of these atomic orbitals (AO), formed with the eigenvector coefficients. Let I_r denote the ionization potential for each site (all I_r are the same if all sites are carbons), then for carbon $I_r = I_C$ = 11.54 eV (lit.[5,12]).

The Hückel matrix is given by

$$H_{rs} = -I_r \, \delta_{rs} - \beta_{rs}(1 - \delta_{rs}) \,. \tag{8}$$

Note that in all cases of B-phase chains with saturating CH_2 groups at the terminal rings, the indices $M + 1$ and $M + 2$ ($M = 6N$) of the two additional carbons bound to carbon 6 in ring 1 and to carbon 3 in ring N have to be included. The one-electron integrals $\beta_{rs} = \beta_{(I-1)6+i;(J-1)6+j}$ are defined only between bonded carbon atoms via the change in the respective bond length ΔR_{rs}:

$$\beta_{ij}^{IJ} = \beta_{rs} = f_{rs}\beta_o \mathrm{e}^{-\alpha_o \Delta R_{rs}}$$

$$\Delta R_{rs} = R_{rs} - R_o^{=} = R_{ij}^{IJ} - R_o^{=}$$

$$f_{rs} = f_{(I-1)6+i;(J-1)6+j} =$$

$$= \delta_{IJ}[\delta_{j,i-1}(1 - \delta_{i1}) + \delta_{i1}\delta_{j6} + \delta_{j,i+1}(1 - \delta_{i6}) + \delta_{i6}\delta_{j1}] +$$

$$+ \delta_{J,I+1}(1 - \delta_{IN})[\delta_{i3}\delta_{j6}\cos^2(\Phi_{I+1} - \Phi_I)] +$$

$$+ \delta_{J,I-1}(1 - \delta_{I1})[\delta_{i6}\delta_{j3}\cos^2(\Phi_I - \Phi_{I-1})] \,. \tag{9}$$

Thus in terms of the explicit indices we have

$$\beta_{rs} = f_{rs}\beta_o \mathrm{e}^{-\alpha_o \Delta R_{rs}} = f_{rs}\beta_o \mathrm{e}^{-\alpha_o (R_{rs} - R_o^{=})} =$$

$$= f_{rs}\beta_o \mathrm{e}^{-\alpha_o (R_{ij}^{IJ} - R_o^{=})} \,. \tag{10}$$

For *trans*-polyacetylene $\beta_o = 2.5$ eV and $\alpha_o = 1.896$ Å^{-1} (taking into account the projected geometry used by SSH[1]) and for the length of a C–C bond in an equidistant, i.e. metallic chain, $R_o^{=} = 1.40$ Å can be chosen[5,37,38]. These numbers probably would have to be fixed newly for poly(*p*-phenylene) because the one-electron integrals are based on the projection of bond lengths on the chain axes of tPA while ours, in contrast to the SSH model, are based on actual C–C bond lengths. R_{rs} is the distance between carbon atoms r and s, written as R_{ij}^{IJ} for carbons i in ring I and j in ring J, thus $r = (I - 1)6 + i$ and $s = (J - 1)6 + j$ (the additional carbon at ring #1 for B phase has an index $6N + 1$, the additional carbon at ring #N for B phase has an index $6N + 2$).

P is the charge density bond order matrix, built from the orbital eigenvector coefficients and the occupation numbers of the orbitals:

$$P_{rs} = \sum_{i=1}^{M'} (o_i^{\alpha} + o_i^{\beta})\, c_{ir}\, c_{is} \tag{11}$$

o_i^{σ} is the occupation number of orbital i for spin σ (0 or 1).

The total π-electron energy is then

$$E_{\pi} = \sum_{r,s=1}^{M'} H_{rs} P_{rs} = \sum_{i=1}^{M'} (o_i^{\alpha} + o_i^{\beta})\, \varepsilon_i \tag{12}$$

where M' is equal to $6N$ in a chain containing only N rings, but equal to $6N + 2$ in a chain containing two CH_2 groups.

The gradients for a fully variationally solved Hückel problem can be obtained by differentiating all the integrals in the Hückel-matrix elements, but not the P-matrix elements, although they depend via the eigenvector coefficients implicitely on geometry: it was shown that the occurring sums of their derivatives sum up to exactly zero[38,39] due to the ZDO approximation, while in case of an overlap matrix other than ***I***, they yield sums of derivatives of overlap matrix elements. Thus the π-electron energy in some more detail is:

$$E_{\pi} = -M' I_c - \sum_{rs} \beta_{rs} P_{rs} (1 - \delta_{rs})\,. \tag{13}$$

Since the one-electron integrals are defined between each pair of carbons, it is now only necessary to detail the sum over the one-electron integrals a bit further (for P-matrix elements the carbon numbers within a ring are taken as indices, the ring numbers are written in bracketts). Note that $P_{ij}(I,J) = P_{ji}(J,I)$ applies

$$\begin{aligned} -\sum_{rs} \beta_{rs} P_{rs} (1 - \delta_{rs}) = \\ = -\sum_{I=1}^{N} \left[\sum_{i=2}^{6} \beta_{i,i-1}^{II} P_{i,i-1}(I,I) + (\beta_{16}^{II} + \beta_{61}^{II}) P_{16}(I,I) + \sum_{i=1}^{5} \beta_{i,i+1}^{II} P_{i,i+1}(I,I) \right] - \\ - \sum_{I=1}^{N-1} \beta_{36}^{I,I+1} P_{36}(I,I+1) - \sum_{I=2}^{N} \beta_{63}^{I,I-1} P_{63}(I,I-1)\,. \end{aligned} \tag{14}$$

To obtain derivatives of the energy with respect to the *q*-s we have already mentioned that in all these terms only the integrals need to be differentiated, not the P-matrix elements. Differentiation of the one-electron integrals yields

$$\frac{\partial \beta_{ij}^{IJ}}{\partial q_L} = -\alpha_o f_{ij}^{IJ} e^{-\alpha_o (R_{ij}^{IJ} - R_o^{=})} \left(\frac{\partial R_{ij}^{IJ}}{\partial q_I} \delta_{IL} + \frac{\partial R_{ij}^{IJ}}{\partial q_J} \delta_{JL} \right) =$$

$$= -\alpha_o \beta_{ij}^{IJ} \left(\frac{\partial R_{ij}^{IJ}}{\partial q_I} \delta_{IL} + \frac{\partial R_{ij}^{IJ}}{\partial q_J} \delta_{JL} \right). \qquad (15)$$

Thus the derivatives of the π-electron energy can be written as

$$\frac{\partial E_\pi}{\partial q_J} = -\sum_{rs} \frac{\partial \beta_{rs}}{\partial q_J} P_{rs}(1 - \delta_{rs}) . \qquad (16)$$

Therefore we have

$$-\sum_{rs} \frac{\partial \beta_{rs}}{\partial q_L} P_{rs}^{\sigma}(1 - \delta_{rs}) =$$

$$= \alpha_o \sum_{I=1}^{N} \left[\sum_{i=2}^{6} \beta_{i,i-1}^{II} P_{i,i-1}^{\sigma}(I,I) \frac{\partial R_{i,i-1}^{II}}{\partial q_I} + \right.$$

$$+ \beta_{16}^{II} P_{16}^{\sigma}(I,I) \frac{\partial R_{16}^{II}}{\partial q_I} + \beta_{61}^{II} P_{61}^{\sigma}(I,I) \frac{\partial R_{61}^{II}}{\partial q_I} +$$

$$\left. + \sum_{i=1}^{5} \beta_{i,i+1}^{II} P_{i,i+1}^{\sigma}(I,I) \frac{\partial R_{i,i+1}^{II}}{\partial q_I} \right] \delta_{IL} +$$

$$+ \alpha_o \sum_{I=1}^{N-1} \beta_{36}^{I,I+1} P_{36}^{\sigma}(I,I+1) \left(\frac{\partial R_{36}^{I,I+1}}{\partial q_I} \delta_{IL} + \frac{\partial R_{36}^{I,I+1}}{\partial q_{I+1}} \delta_{I+1,L} \right) +$$

$$+ \alpha_o \sum_{I=2}^{N} \beta_{63}^{I,I-1} P_{63}^{\sigma}(I,I-1) \left(\frac{\partial R_{63}^{I,I-1}}{\partial q_I} \delta_{IL} + \frac{\partial R_{63}^{I,I-1}}{\partial q_{I-1}} \delta_{I-1,L} \right) \qquad (17)$$

which finally, after performing the sum over I, gives

$$-\sum_{rs}\frac{\partial\beta_{rs}}{\partial q_J}P_{rs}(1-\delta_{rs}) =$$

$$\alpha_o\left[\sum_{i=2}^{6}\beta_{i,i-1}^{JJ}P_{i,i-1}(J,J)\frac{\partial R_{i,i-1}^{JJ}}{\partial q_J} +\right.$$

$$+\beta_{16}^{JJ}P_{16}(J,J)\frac{\partial R_{16}^{JJ}}{\partial q_J}+\beta_{61}^{JJ}P_{61}(J,J)\frac{\partial R_{61}^{JJ}}{\partial q_J}+$$

$$\left.+\sum_{i=1}^{5}\beta_{i,i+1}^{JJ}P_{i,i+1}(J,J)\frac{\partial R_{i,i+1}^{JJ}}{\partial q_J}\right]+$$

$$+\alpha_o\left(\beta_{36}^{J,J+1}P_{36}(J,J+1)\frac{\partial R_{36}^{J,J+1}}{\partial q_J}+\beta_{63}^{J+1,J}P_{63}(J+1,J)\frac{\partial R_{63}^{J+1,J}}{\partial q_J}\right)(1-\delta_{JN})+$$

$$+\alpha_o\left(\beta_{63}^{J,J-1}P_{63}(J,J-1)\frac{\partial R_{63}^{J,J-1}}{\partial q_J}+\beta_{36}^{J-1,J}P_{36}(J-1,J)\frac{\partial R_{36}^{J-1,J}}{\partial q_J}\right)(1-\delta_{J1})\,. \qquad (18)$$

As last step for the calculation of derivatives we have to turn to the Φ-s now. We have to look only at the terms which contain the bridge one-electron integrals. Because we have to note that a ring rotation does not change the intraring bond lengths, and thus the derivatives of intraring β-s with respect to any ring rotation angle Φ_J simply vanish. The other β-s between rings are only those for the bridge bonds. Again the rotation of rings does not change the lengths of these bonds; however, β depends on Φ via the $\cos^2$ factor which takes into account the rotation relative to each other of the two p orbitals, forming the bridge π-bond. Thus

$$\frac{\partial\beta_{ij}^{IJ}}{\partial\Phi_L}=-\beta_o\,e^{-\alpha\Delta R_{ij}^{I,I+1}}\,2\cos(\Phi_{I+1}-\Phi_I)\sin(\Phi_{I+1}-\Phi_I)(\delta_{I+1,L}-\delta_{IL})\,. \qquad (19)$$

Then the complete term in E_π becomes

$$-\sum_{rs}\frac{\partial\beta_{rs}}{\partial\Phi_L}P_{rs}(1-\delta_{rs}) =$$

$$= \sum_{I=1}^{N-1}\beta_o e^{-\alpha\Delta R_{3,6}^{I,I+1}} P_{36}(I,I+1)\ 2\cos(\Phi_{I+1}-\Phi_I)\sin(\Phi_{I+1}-\Phi_I)(\delta_{I+1,L}-\delta_{IL}) +$$

$$+ \sum_{I=2}^{N}\beta_o e^{-\alpha\Delta R_{6,3}^{I,I-1}} P_{63}(I,I-1)\ 2\cos(\Phi_I-\Phi_{I-1})\sin(\Phi_I-\Phi_{I-1})(\delta_{I,L}-\delta_{I-1,L}) \quad (20)$$

and finally

$$-\sum_{rs}\frac{\partial\beta_{rs}}{\partial\Phi_J}P_{rs}(1-\delta_{rs}) =$$

$$= \Big(e^{-\alpha\Delta R_{3,6}^{J-1,J}} P_{36}(J-1,J)\cos(\Phi_J-\Phi_{J-1})\sin(\Phi_J-\Phi_{J-1}) -$$

$$- e^{-\alpha\Delta R_{3,6}^{J,J+1}} P_{36}(J,J+1)\cos(\Phi_{J+1}-\Phi_J)\sin(\Phi_{J+1}-\Phi_J) +$$

$$+ e^{-\alpha\Delta R_{6,3}^{J,J-1}} P_{63}(J,J-1)\cos(\Phi_J-\Phi_{J-1})\sin(\Phi_J-\Phi_{J-1}) -$$

$$- e^{-\alpha\Delta R_{6,3}^{J+1,J}} P_{63}(J+1,J)\cos(\Phi_{J+1}-\Phi_J)\sin(\Phi_{J+1}-\Phi_J)\Big)\beta_o \ . \quad (21)$$

II.2.2. Parameters

Since the potential surfaces given in[36] were based on another geometry than the one we use here, we had to recalculate a few A and B-phase dimers, using the Gaussian98[40] program to perform DFT/B3LYP calculations (density functional theory/Becke-3 exchange, Lee–Yang–Parr correlation potential) with a valence split atomic basis set augmented with d functions on heavy atoms and p functions on hydrogens. We calculated energy differences between the A-phase minimum [$E_A(q = +1$ Å)] and two other A-phase geometries (q = 0, Φ = 90° and $\Phi/2$) and between the B phase minimum [$E_B(q = -1$ Å)] and two other B phase geometries (q = 0, Φ = 0° and $\Phi/2$). Then we did a least-square fit to determine optimum parameters, using the σ-electron potential model A (same harmonic oscillator for all C–C σ-bonds) and model C (two sets of harmonic oscillators for intra- and inter-

ring C–C σ-bonds) as described below. To this end we calculated these energy differences with 50 different values of β_o, between 0.0001 and 25 eV, and at each of the β values we used 50 values of α_o between 0.0001 and 25 $Å^{-1}$ and determined the parameter values, where the smallest root-mean-square deviation (rms) between the DFT and the Hückel energy differences occurred. Then the procedure was repeated around the minimum with a step length of 0.1 eV and 0.1 $Å^{-1}$, respectively. Finally we repeated that again around the new minimum, now with a step length of 0.01 eV and 0.01 $Å^{-1}$, respectively. For model A we obtained in this way a minimal rms of 0.30 kcal/mol at β_o = 2.12 eV and α_o = 3.41 $Å^{-1}$, while for model C we obtained a minimal rms of 0.26 kcal/mol at β_o = 2.44 eV and α_o = 2.91 $Å^{-1}$. The individual energies are listed in Table II.

TABLE II

Total DFT energies (in Hartrees, H) for the six dimers used in the parametrization, together with the energy differences (detailed in footnote[a]) as calculated for the DFT values (both in H and kcal/mol) and by the Hückel method at the respective minimum rms values, calculated with σ-potential model A, as well as with σ-potential model C

DFT energies of the dimers				
Dimer	*E*/H			
A (q = +1 Å, $\Phi = \Phi_o$)	–463.321939393			
A (q = 0, $\Phi = \Phi_o/2$)	–463.314092674			
A (q = 0, Φ = 90°)	–463.310128113			
B (q = –1 Å, Φ = 0)	–540.667976863			
B (q = 0, $\Phi = \Phi_o/2$)	–540.653990266			
B (q = 0, Φ = 0)	–540.657053953			
Energy differences				
i^a	ΔE_i(DFT)/H	ΔE_i(DFT)/kcal/mol	ΔE_i(A)/kcal/mol	ΔE_i(C)/kcal/mol
1	-7.846719×10^{-3}	–4.92	–4.65	–4.47
2	–0.01398660	–8.78	–8.72	–8.99
3	–0.01181128	–7.41	–7.87	–7.51
4	–0.01092291	–6.85	–6.58	–6.75

[a] ΔE_1 = A (q = +1 Å, $\Phi = \Phi_o$) – A (q = 0, $\Phi = \Phi_o/2$); ΔE_2 = B (q = –1 Å, Φ = 0) – B (q = 0, $\Phi = \Phi_o/2$); ΔE_3 = A (q = +1 Å, $\Phi = \Phi_o$) – A (q = 0, Φ = 90°); ΔE_4 = B (q = –1 Å, Φ = 0) – B (q = 0, Φ = 0); (DFT) denotes DFT values, (A) are at minimum rms for potential model A, (C) are at minimum rms for potential model C.

The Table shows that the agreement between the DFT values and those calculated with the two potentials is in both cases rather satisfactory. Let us turn now to the different potential models tested in this work.

II.3. The σ-Electron Potentials

The total potential energy consists of three parts, where the analytical potential terms in V_σ are assumed to describe contributions due to the σ electrons (V_σ^σ) and due to the repulsion between the hydrogen atoms near to the bridge bonds between the rings (V_σ^Φ). The third part consists of the π-electron energy (E_π), which, as discussed above, in our preliminary model is calculated with the Hückel hamiltonian:

$$V = V_\sigma^\sigma + V_\sigma^\Phi + E_\pi = V_\sigma + E_\pi \ . \qquad (22)$$

The following subsections describe the σ-terms as well as their derivatives with respect to the degrees of freedom. Further we show how the parameters entering the terms can be determined. As it will be described in detail, we had to try out several different *Ansätze* for the σ-electron potential model, due to difficulties in getting the right minima and the parameters converging with the number of rings in a chain, *N*. We suggest that this shortcoming might be due to our use of a Hückel-type model for the π-electrons.

To make the suspected form of the carriers in poly(*p*-phenylene) plausible, we show idealized sketches of poly(*p*-phenylene) chains. Those are idealized, because in the real material changes between the aromatic (A) and the quinoid (B) phases should be gradual, while in the sketches they are localized basically in one carbon atom each. Figure 2 shows a neutral polaron structure in a chain (triplet in this example), which has two unpaired electrons at its two ends. They would not be stable because the B-phase segment between the isolated electrons has a higher energy than the A phase. Thus such a neutral structure would simply relax to the aromatic phase

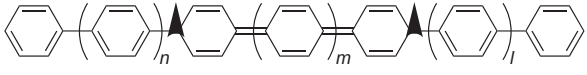

FIG. 2
Sketch of a neutral polaron structure (triplet) in a poly(*p*-phenylene) chain (note that the changes from A to B phase and from B to A phase at the ends of the polaron are idealized to a zero width)

throughout. In Fig. 3 one of the unpaired electrons is removed, to give a polaron, which is singly charged, in the example positive, and carries an unpaired spin, both delocalized over the B-phase segment (which is there-

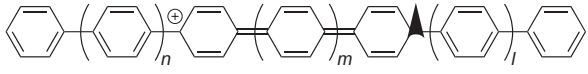

FIG. 3
Sketch of a positively charged polaron structure with an unpaired spin in a poly(*p*-phenylene) chain (note that the changes from A to B phase and from B to A phase at the ends of the polaron are idealized to a zero width)

fore not fully developed). Since the charge transport in doped poly(*p*-phenylene) involves no spin transport, in the actual charge carriers the second unpaired electron is also removed to form a positively charged bipolaron as shown in Fig. 4.

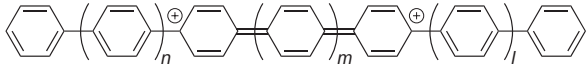

FIG. 4
Sketch of a positively charged, spinless bipolaron structure in a poly(*p*-phenylene) chain (note that the changes from A to B phase and from B to A phase at the ends of the bipolaron are idealized to a zero width)

The length of the B-segment in a bipolaron would be determined by the balance of two forces. The repulsion between the two like charges favors a long B-phase segment, while the higher energy of the B phase favors a short one. The positive charge occurs in cases of p-type doping and would be negative if n-type doping is investigated.

II.3.1. The σ-Electron Potential Model A

The simplest, most obvious choice of a potential to describe the σ-electron energies requires two parts, one dealing with the lengths of σ bonds (V_σ^σ) and another one describing the repulsion between the hydrogen atoms near to the bridging bonds, which also originates mostly from the σ electrons of CH single bonds; however, their distance depends on the relative rotation angles between two neighboring rings (V_σ^Φ):

$$V_\sigma = V_\sigma^\sigma + V_\sigma^\Phi . \qquad (23)$$

Thus V_σ^σ is written in terms of the bond distances in and between the rings, and in model A we assume one and the same harmonic oscillator for the description of all C–C σ-bonds:

$$V_\sigma^\sigma = \frac{1}{2} K_\sigma \sum_{J=1}^{N} \left\{ \sum_{i=1}^{5} (R_{i,i+1}^{J,J} - R_o)^2 + (R_{6,1}^{J,J} - R_o)^2 + (R_{3,6}^{J,J+1} - R_o)^2 (1 - \delta_{J,N}) \right\}. \quad (24)$$

Here $R_{i,j}^{I,J}$ denotes the distance between carbon atom i in ring I and carbon atom j in ring J. K_σ is the force constant for C–C σ-bonds, while R_o is the equilibrium distance for C–C σ-bonds. These are the two parameters which have to be determined to fix the total energy minima at phases A and B. In case of terminal B-phase rings one has to add 2 terms for the additional CH_2 groups instead of hydrogen in the case of aromatic terminal rings:

$$V_\sigma^\sigma + \frac{1}{2} K_\sigma \left[(\sqrt{(x_{6N+1}(q_{N+1}) - x_6^1)^2} - R_o)^2 + (\sqrt{(x_3^N - x_{6N+2}(q_{N+2}))^2} - R_o)^2 \right] \quad (25)$$

where the first term contains the deviation of the bond length between the additional carbon $6N + 1$ and carbon 6 in the first ring and the equilibrium σ-bond length, while the second term contains the same for carbon 3 in the last ring N and the additional carbon $6N + 2$.

For the second part of the potential we suggested in[36] to use $\cos^2$ terms in the relative rotation angles between neighboring rings, which oscillate between 0 at the largest distance between the hydrogens and 1 at the smallest distance between the hydrogens of two neighboring rings. Thus we expect that Φ_o turns out to approximately vanish, because $\cos^2$ has already the correct symmetry dependence on the Φ-s. The potential becomes

$$V_\sigma^\Phi = V_\Phi \sum_{J=1}^{N-1} \cos^2(\Phi_{J+1} - \Phi_J - \Phi_o). \quad (26)$$

To fix the constants, for a given chain length of N rings, two systems have to be calculated, using our model:

1. The aromatic A phase, with $6N$ carbon atoms, which should be a minimum of the total energy for $q_J = +1$ Å and $\Phi_J = (J - 1)\Phi_o^A$; and

2. The quinoid B phase, with $6N + 2$ carbon atoms, which should be another minimum of the total energy for $q_J = -1$ Å and $\Phi_J = 0°$.

Thus for uniform $q_J = q$ we have (E_t denotes total energy)

$$\frac{\partial E_t}{\partial q} = \sum_{J=1}^{N} \frac{\partial E_t}{\partial q_J} \frac{\partial q_J}{\partial q} = \sum_J \frac{\partial E_t}{\partial q_J} \tag{27}$$

while for $\Phi_J = (J - 1)\Phi$ we have

$$\frac{\partial E_t}{\partial \Phi} = \sum_{J=1}^{N} \frac{\partial E_t}{\partial \Phi_J} \frac{\partial \Phi_J}{\partial \Phi} = \sum_J (J-1) \frac{\partial E_t}{\partial \Phi_J} . \tag{28}$$

Thus for the chain in A phase the conditions

$$\frac{\partial E_t^A}{\partial q}\Big|_{q=1\,\text{Å};\,\Phi=\Phi_o^A} = \frac{\partial E_t^A}{\partial \Phi}\Big|_{q=1\,\text{Å};\,\Phi=\Phi_o^A} = 0 \tag{29}$$

have to be fulfilled. For the B-phase calculation one has to add the two terminal CH_2 groups $M + 1$ and $M + 2$ ($M = 6N$) and the conditions

$$\frac{\partial E_t^B}{\partial q}\Big|_{q=1\,\text{Å};\,\Phi=0°} = \frac{\partial E_t^B}{\partial \Phi}\Big|_{q=1\,\text{Å};\,\Phi=0°} = 0 \tag{30}$$

must be fulfilled. The corresponding π-electron energies will be denoted as E_π^A and E_π^B.

Since V_σ^σ depends only on bond length changes which do not depend on ring rotations, its derivatives with respect to Φ_J vanish and since V_σ^Φ depends only on Φ_J, its derivatives with respect to q_J vanish. Thus the above four conditions will yield two decoupled systems of two equations each, one in K_σ and R_o and the other one in V_Φ and Φ_o (in the case of the $\cos^2$ form) only.

Unfortunately, it turned out that with the $\cos^2$ potential term it is impossible to ensure minima in A and B for all chain lengths. The potential should represent non-bonded interactions between the hydrogen atoms at the bridge carbons. Thus we turned to consider a potential of a London type instead:

$$V_\sigma^\Phi = V_\Phi \sum_{J=1}^{N-1} \left[1 + \alpha \sin^2(\Delta\phi_J)\right]^{-n}$$

$$\Delta\phi_J = \phi_{J+1} - \phi_J ; \quad \alpha = \frac{R_{HH}^{90°}}{R_{HH}^B} - 1 . \tag{31}$$

From a point charge geometry it would follow that α should be equal to 0.58033. However, it turned out that to ensure minima in A and B and $n = 6$ (London-type force), $\alpha = 0.3$ has to be chosen. Then minima can be ensured in the right angles for the respective A and B form for all chain lengths considered. This we could ensure, using the π-electron energy derivatives given by our program. A smaller α value than the theoretical one makes physical sense because the electrons themselves interact repulsively already at smaller distances than the point charges.

For the derivatives of the potential we need the derivatives of the bond distances. For the distance between two atoms i and j in rings I and J we have

$$R_{i,j}^{I,J} = \left[\sum_{\mu=1}^{3} (\boldsymbol{R}_{Ii} - \boldsymbol{R}_{Jj})_{\mu}^{2} \right]^{1/2} =$$

$$= \left[\sum_{\mu} \left\{ \boldsymbol{D}_x(\Phi_I)[\boldsymbol{R}_i + \tfrac{1}{2}(1\text{Å} - q_I)\,\boldsymbol{\Delta}_i] - \right.\right.$$

$$\left.\left. - \boldsymbol{D}_x(\Phi_J)[\boldsymbol{R}_j + \tfrac{1}{2}(1\text{Å} - q_J)\,\boldsymbol{\Delta}_j] + (I - J)\, t\boldsymbol{e}_x \right\}_{\mu}^{2} \right]^{1/2} . \qquad (32)$$

Thus derivatives with respect to the q-s are

$$\frac{\partial R_{i,j}^{I,J}}{\partial q_I} = \frac{1}{2R_{i,j}^{I,J}} 2 \sum_{\mu} [\boldsymbol{R}_{Ii} - \boldsymbol{R}_{Jj}]_{\mu} [-\tfrac{1}{2}\boldsymbol{D}_x(\Phi_I)\,\boldsymbol{\Delta}_i]_{\mu}$$

$$\frac{\partial R_{i,j}^{I,J}}{\partial q_J} = \frac{1}{R_{i,j}^{I,J}} \sum_{\mu} [\boldsymbol{R}_{Ii} - \boldsymbol{R}_{Jj}]_{\mu} [\tfrac{1}{2}\boldsymbol{D}_x(\Phi_J)\,\boldsymbol{\Delta}_j]_{\mu}$$

$$\frac{\partial R_{i,j}^{J,J}}{\partial q_J} = \frac{1}{R_{i,j}^{J,J}} \sum_{\mu} [\boldsymbol{R}_{Ji} - \boldsymbol{R}_{Jj}]_{\mu} [\tfrac{1}{2}\boldsymbol{D}_x(\Phi_J)\,(-\boldsymbol{\Delta}_i + \boldsymbol{\Delta}_j)]_{\mu}$$

$$\frac{\partial R_{i,j}^{J,J+1}}{\partial q_L} = \frac{1}{R_{i,j}^{J,J+1}} \sum_{\mu} [\boldsymbol{R}_{Ji} - \boldsymbol{R}_{J+1,j}]_{\mu} [-\tfrac{1}{2}\boldsymbol{D}_x(\Phi_J)\,\boldsymbol{\Delta}_i\,\delta_{J,L} +$$

$$+ \tfrac{1}{2}\,\boldsymbol{D}_x(\Phi_{J+1})\,\boldsymbol{\Delta}_j\,\delta_{J+1,L}]_{\mu} . \qquad (33)$$

For the determination of K_σ and R_o we need now the derivatives of V_σ^σ with respect first to q_L and then for uniform $q_L = q$

$$\frac{\partial V_\sigma^\sigma}{\partial q_L} = \frac{1}{2} K_\sigma \; 2 \sum_{J=1}^{N} \left[\sum_{i=1}^{5} (R_{i,i+1}^{J,J} - R_o) \frac{\partial R_{i,i+1}^{J,J}}{\partial q_J} \delta_{JL} + \right.$$

$$\left. + (R_{6,1}^{J,J} - R_o) \frac{\partial R_{6,1}^{J,J}}{\partial q_J} \delta_{JL} \right] +$$

$$+ K_\sigma \sum_{J=1}^{N-1} \left[(R_{3,6}^{J,J+1} - R_o) \left(\frac{\partial R_{3,6}^{J,J+1}}{\partial q_J} \delta_{JL} + \frac{\partial R_{3,6}^{J,J+1}}{\partial q_{J+1}} \delta_{J+1,L} \right) \right]. \qquad (34)$$

Thus after the summation over J is performed, we arrive at

$$\frac{\partial V_\sigma^\sigma}{\partial q_L} = K_\sigma \left\{ \sum_{i=1}^{5} (R_{i,i+1}^{L,L} - R_o) \frac{\partial R_{i,i+1}^{L,L}}{\partial q_L} + (R_{6,1}^{L,L} - R_o) \frac{\partial R_{6,1}^{L,L}}{\partial q_L} + \right.$$

$$\left. + \left[(R_{3,6}^{L,L+1} - R_o) \frac{\partial R_{3,6}^{L,L+1}}{\partial q_L} (1 - \delta_{LN}) + (R_{3,6}^{L-1,L} - R_o) \frac{\partial R_{3,6}^{L-1,L}}{\partial q_L} (1 - \delta_{L1}) \right] \right\}. \qquad (35)$$

Since the geometry is a uniform one with $q_J = q$, we have

$$\frac{\partial V_\sigma^\sigma}{\partial q} = \sum_{L=1}^{N} \frac{\partial V_\sigma^\sigma}{\partial q_L} \frac{\partial q_L}{\partial q} = \sum_{L=1}^{N} \frac{\partial V_\sigma^\sigma}{\partial q_L}. \qquad (36)$$

Furthermore, since V_σ^Φ does not depend on q and thus its derivative with respect to q vanishes, the derivative of the total energy E_t is

$$\frac{\partial E_t}{\partial q} = \frac{\partial V_\sigma^\sigma}{\partial q} + \frac{\partial E_\pi}{\partial q} \qquad (37)$$

where the calculation of the derivative of the π-electron energy was described in the previous subsection.

To get a separation of R_o and K_σ we write down the following two expressions:

$$P = \sum_{L=1}^{N} \left[\sum_{i=1}^{5} R_{i,i+1}^{L,L} \frac{\partial R_{i,i+1}^{L,L}}{\partial q_L} + R_{6,1}^{L,L} \frac{\partial R_{6,1}^{L,L}}{\partial q_L} + \right.$$

$$+\left(R_{3,6}^{L,L+1}\frac{\partial R_{3,6}^{L,L+1}}{\partial q_L}(1-\delta_{LN})+R_{3,6}^{L-1,L}\frac{\partial R_{3,6}^{L-1,L}}{\partial q_L}(1-\delta_{L1})\right)\Bigg]$$

$$Q=\sum_{L=1}^{N}\Bigg[\sum_{i=1}^{5}\frac{\partial R_{i,i+1}^{L,L}}{\partial q_L}+\frac{\partial R_{6,1}^{L,L}}{\partial q_L}+$$

$$+\left(\frac{\partial R_{3,6}^{L,L+1}}{\partial q_L}(1-\delta_{LN})+\frac{\partial R_{3,6}^{L-1,L}}{\partial q_L}(1-\delta_{L1})\right)\Bigg]. \qquad (38)$$

Thus we have to calculate a chain with N rings in the aromatic A-phase minimum (q_J = +1 Å, $\Phi_J = (J-1)\Phi_o^{\mathrm{A}}$) to get E_π^{A} and, by using this geometry, to calculate P^{A} and Q^{A}. Subsequently we have to calculate a chain with N rings plus two additional CH_2 units at each terminal ring in the quinoid B-phase minimum (q_J = –1 Å, $\Phi_J = \Phi = 0°$) to get E_π^{B} and, by using this geometry, to calculate P^{B} and Q^{B}. In the latter case for each terminal CH_2 unit an additional term has to be added in P^{B} and Q^{B}. Then we can set up the minimum conditions

$$\frac{\partial E_{\mathrm{t}}^{\mathrm{A}}}{\partial q}=\frac{\partial V_\sigma^{\sigma,\mathrm{A}}}{\partial q}+\frac{\partial E_\pi^{\mathrm{A}}}{\partial q}=0$$

$$\frac{\partial E_{\mathrm{t}}^{\mathrm{B}}}{\partial q}=\frac{\partial V_\sigma^{\sigma,\mathrm{B}}}{\partial q}+\frac{\partial E_\pi^{\mathrm{B}}}{\partial q}=0 \qquad (39)$$

where superscripts A and B denote that the derivatives have to be taken at the corresponding minimum geometries. This leads to the system of equations

$$K_\sigma P^{\mathrm{A}}-K_\sigma R_o Q^{\mathrm{A}}+\frac{\partial E_\pi^{\mathrm{A}}}{\partial q}=0$$

$$K_\sigma P^{\mathrm{B}}-K_\sigma R_o Q^{\mathrm{B}}+\frac{\partial E_\pi^{\mathrm{B}}}{\partial q}=0\,. \qquad (40)$$

Since the σ-electron potential is a quadratic form of the q_J-s, one hopes that these conditions are sufficient to ensure minima at A and B. The first equation yields

$$K_\sigma = -\frac{\partial E_\pi^A}{\partial q}[P^A - R_o Q^A]^{-1}. \tag{41}$$

Substitution into the second equation gives

$$-\frac{P^B - R_o Q^B}{P^A - R_o Q^A}\frac{\partial E_\pi^A}{\partial q} + \frac{\partial E_\pi^B}{\partial q} = 0 \tag{42}$$

and therefore

$$R_o = \frac{P^B \dfrac{\partial E_\pi^A}{\partial q} - P^A \dfrac{\partial E_\pi^B}{\partial q}}{Q^B \dfrac{\partial E_\pi^A}{\partial q} - Q^A \dfrac{\partial E_\pi^B}{\partial q}} \tag{43}$$

and

$$K_\sigma = \frac{\partial E_\pi^A}{\partial q}\left[\frac{P^B \dfrac{\partial E_\pi^A}{\partial q} - P^A \dfrac{\partial E_\pi^B}{\partial q}}{Q^B \dfrac{\partial E_\pi^A}{\partial q} - Q^A \dfrac{\partial E_\pi^B}{\partial q}} Q^A - P^A\right]^{-1}. \tag{44}$$

For the determination of V_Φ we have to look at the derivatives of V_σ^Φ, since, as mentioned above, the derivative of V_σ^σ with respect to the Φ-s vanishes, because it depends only on bond lengths which do not change due to rotations of the rings. This holds, because only intraring bonds and the bridge bond along the rotation axis enter. Our numerical calculations have shown that the derivatives of the π-electron energies with respect to the Φ-s for all chain lengths up to $N = 200$ vanish for B phase. Thus, for the derivative of the total energies to vanish as well, that of the Φ-dependent part of the σ potential must vanish either in B phase. For a uniform rotation angle Φ between two consecutive rings (or between a CH_2 group and the ring bound to it in B phase) throughout the chain, we have

$$V_\sigma^\phi = V_\phi(N-1)[1+\alpha \sin^2 \phi]^{-n}. \tag{45}$$

Since in the case of B phase we have for this angle $\Phi = 0$:

$$V_\sigma^{\phi,\mathrm{B}} = V_\phi(N+1) \Rightarrow \frac{\partial V_\sigma^{\phi,\mathrm{B}}}{\partial\phi}|_{\phi=0} = 0$$

$$\frac{\partial E_\pi^{\mathrm{B}}}{\partial\phi} = 0 \;\forall\; N \Rightarrow \frac{\partial E_\mathrm{t}^{\mathrm{B}}}{\partial\phi}|_{\phi=0} = 0 \;\forall\; N\,. \qquad (46)$$

Further, for A phase we have

$$V_\sigma^{\phi,\mathrm{A}} = V_\phi(N-1)[1+\alpha\sin^2\phi]^{-n} \Rightarrow$$
$$\Rightarrow \frac{\partial V_\sigma^{\phi,\mathrm{A}}}{\partial\phi}|_{\phi=\phi_\mathrm{o}^\mathrm{A}} = -nV_\phi(N-1)[1+\alpha\sin^2\phi_\mathrm{o}^\mathrm{A}]^{-n-1}\; 2\alpha\sin\phi_\mathrm{o}^\mathrm{A}\cos\phi_\mathrm{o}^\mathrm{A} \qquad (47)$$

and for a minimum in this phase we need at least

$$\frac{\partial E_\mathrm{t}^{\mathrm{A}}}{\partial\phi}|_{\phi=\phi_\mathrm{o}^\mathrm{A}} = \frac{\partial V_\sigma^{\phi,\mathrm{A}}}{\partial\phi}|_{\phi=\phi_\mathrm{o}^\mathrm{A}} + \frac{\partial E_\pi^{\mathrm{A}}}{\partial\phi} = 0 \qquad (48)$$

and thus for our potential constant

$$V_\phi = \frac{\frac{\partial E_\pi^{\mathrm{A}}}{\partial\phi}[1+\alpha\sin^2\phi_\mathrm{o}^\mathrm{A}]^{n+1}}{n(N-1)\;2\alpha\sin\phi_\mathrm{o}^\mathrm{A}\;\cos\phi_\mathrm{o}^\mathrm{A}} \qquad (49)$$

where we decided to use $n = 6$.

We have calculated the potential constants for a few chain lengths between $N = 2$ and $N = 150$. Note that in these calculations with model A we used $\beta_\mathrm{o} = 2.20$ eV and $\alpha_\mathrm{o} = 3.32$ Å^{-1}, which were determined only from three of the four dimer energy differences calculated with DFT. We checked whether the extremes are minima or maybe maxima in A and B. When using two CH_2 groups, variable in q and Φ, at the B-phase chains, we found that for $N = 5$, 10, 20 and 150, B is indeed a maximum with $E^\mathrm{B}(q = -1\text{ Å} + h) - E^\mathrm{B} < 0$ and $E^\mathrm{B}(q = -1\text{ Å} - h) - E^\mathrm{B} < 0$ for $h = 1$ mÅ. Thus we repeated the calculations with CH_2 groups that are fixed, being coplanar to the rings to which they are bound, q being still variables. In this case A and B phases where real minima for all chain lengths. Table III lists the potential constants obtained together with the aromatization energies, being

$$E_{A-B} = \frac{1}{N}[E_A - (E_B + 2I_C + 2\beta_{C=C}(P_{i_1,j_1} + P_{i_2,j_2}) - -K_\sigma(R_{C=C} - R_o)^2 - 2V_\phi)] \quad (50)$$

$$\beta_{C=C} = -\beta_o e^{-\alpha_o (R_{C=C} - R^=)}; \quad \beta_o = 2.20 \text{ eV}; \quad \alpha_o = 3.32 \text{ Å}^{-1}$$

$$R^= = 1.400 \text{ Å}; \quad R_{C=C} = 1.359400 \text{ Å for biphenyl}$$

$$R_{C=C} = 1.363489 \text{ Å for all others } (N > 2)$$

$$i_1 = 6; \quad j_1 = 6N + 1; \quad i_2 = 6(N - 1) + 3; \; j_2 = 6N + 2$$

where $I_C = 11.54$ eV is the ionization potential of carbon and N the number of rings in the chain. Note that we removed as many energy components originating from the CH_2 groups as possible from the B-phase energies since CH_2 groups are not present in A phase.

From the Table it is obvious that neither R_o nor the force constants K_σ converge properly up to $N = 150$. Actually R_o increases to 2.17 Å for $N = 150$, which is far too large to approximate the equilibrium length of a C–C single bond, which should be around $R_o = 1.5$ Å. Both the increasing R_o value as well as the increasing force constant lead to the fact that, although the π-electron energy is negative in all cases, the total energy becomes positive for larger chains. Further the aromatization energy increases rapidly from –2 eV/ring (dimer) to +0.1 meV/ring ($N = 150$). Thus in the latter case, the quinoid phase is slightly more stable than the aromatic one.

TABLE III
The σ potential constants for model A with additional CH_2 groups in B phase, together with the aromatization energies for different numbers of rings N in the chains ($E_t > 0$ for larger N)

N	R_o, Å	K_σ, eV/Å^2	V_Φ, eV	E_{A-B}, meV/ring
2	1.496	100.61	0.730	–1973.9
3	1.528	91.89	0.814	–1290.9
5	1.621	74.71	0.853	–704.2
10	1.881	57.44	0.876	–217.8
20	2.124	58.02	0.885	–0.6
150	2.169	91.16	0.892	+0.1

To see how this behavior changes when the CH_2 groups in B phase are removed, we repeated the calculations without CH_2 groups in B, already in the determination of the potential constants. In this case the aromatization energy is simply the difference $E_A - E_B$ divided by the number of rings N. The results are given in Table IV.

We can see in the Table IV, first of all, that R_o still approaches a too high value as the chain length increases and thus causes, together with the large force constants, again positive values of the total energy when N increases above 40. As before, V_Φ converges smoothly to its final value, which is comparatively small as expected. However, the aromatization energy is now also converging with N, but is positive throughout. E'_{A-B}, which is the energy difference between aromatic and quinoid phase, if only E_π and V_σ^Φ are included but not the σ part of the potential. This is indeed negative, but then, without including V_σ^σ, the minima in $q = \pm 1$ Å for A and B are not fixed. Obviously one has to look for another way to model the σ-electrons.

TABLE IV

The corresponding values, as in Table III, for model A, but for systems without CH_2 groups in B phase. Note that here E_{A-B} is the simple difference between A- and B-phase energies (minimum positions all checked; $E_t(N > 40) > 0$; $E_\pi + V_\sigma^\Phi < 0$):

$$E_{A-B} = \frac{1}{N}(E_A - E_B); \qquad E'_{A-B} = \frac{1}{N}[E_\pi^A + V_\sigma^{\phi,A} - (E_\pi^B + V_\sigma^{\phi,B})]$$

N	R_o, Å	K_σ, eV/Å^2	V_Φ, eV	E_{A-B}, meV/ring	E'_{A-B}, eV/ring
2	1.624	52.70	0.730	+23.3	–0.6679
3	1.632	59.83	0.814	+28.0	–0.4570
5	1.656	67.48	0.853	+32.2	–0.3322
10	1.718	76.00	0.876	+34.9	–0.2206
20	1.810	83.08	0.885	+36.4	–0.1697
40	1.913	89.20	0.889	+37.3	–0.1442
60	1.968	92.43	0.891	+37.7	–0.1358
80	2.003	94.39	0.891	+37.9	–0.1315
100	2.026	95.73	0.892	+38.0	–0.1290
120	2.044	96.71	0.892	+38.1	–0.1273
140	2.057	97.76	0.892	+38.2	–0.1261
150	2.062	97.77	0.892	+38.3	–0.1256

II.3.2. The σ-Electron Potential Model B

Because of the problems encountered so far, we turned our attention to potentials which do not contain explicit bond lengths, but just the q_K coordinates of a ring *K*. We tried a lot of functional forms, including sinusoidal ones, but the results were always not encouraging. Thus we restrict ourselves to just one type of such potentials. The Φ-part of the potential was kept the same also in model B. In model B the potential is of the type

$$V_\sigma^\sigma = V \sum_K (\eta - q_K)^2 \tag{51}$$

and we decided again to attach no CH_2 groups for the saturation of the outmost left and right rings. Two adjustable constants are again necessary in order to fix the two minima. The minimum conditions for A- and B-phase rings yield

$$V = -\frac{\Delta^-}{4N\text{Å}}; \quad \eta = 1 - 2\frac{\dfrac{\partial E_\pi^\text{A}}{\partial q}}{\Delta^-}$$

$$\Delta^- = \frac{\partial E_\pi^\text{A}}{\partial q} - \frac{\partial E_\pi^\text{B}}{\partial q}\,. \tag{52}$$

The potential parameters together with the aromatization energies are given in Table V for several different chain lengths.

TABLE V

The corresponding values, as in Table III, but here calculated with model B, but for systems without CH_2 groups in B phase. Note that here $E_{A–B}$ is the simple difference between A- and B-phase energies (minimum positions all checked):

$$V_\sigma^\sigma = V \sum_K (\eta - q_K)^2$$

N	η, Å	*V*, eV/Å^2	V_Φ, eV	$E_{A–B}$, eV/ring
2	–1.597	0.10750	0.730	+0.01882
3	–1.358	0.08865	0.814	+0.02456
5	–0.9779	0.08977	0.853	+0.02891
10	–0.6940	0.09087	0.875	+0.03170
20	–0.5540	0.09146	0.885	+0.03301
40	–0.4847	0.09175	0.889	+0.03366
150	–0.4341	0.09197	0.892	+0.03413

The parameter η turns out to be negative throughout. As well as *V* it converges smoothly with the chain length. However, again the quinoid phase is increasingly more stable than the aromatic one with increasing *N*. As we will see below, this behavior allows for no confinement of two like charges and thus we do not want to elaborate here more these types of σ-potentials.

II.3.3. The σ-Electron Potential Model C

It came to our attention that the bonds within the system fall into categories, distinct by symmetry. The interring bonds have another symmetry than the intraring bonds. Although the intraring bonds also can be distinguished into two groups, one with four and the other with two bonds, we decided to ignore this fact because the two minima allow only two variable parameters. However, we have chosen a similar structure of the potential with two different spring constants. In this case we decided to keep R_o = 1.5 Å, a value more appropriate for C–C single bonds, than the ones calculated so far. Thus the changed part of the σ potential is

$$V_\sigma^\sigma = \frac{1}{2}K_\sigma \sum_{\text{intraring}\,\sigma} (R_\sigma - R_o)^2 + \frac{1}{2}K'_\sigma \sum_{\text{interring}\,\sigma} (R_\sigma - R_o)^2 \ . \qquad (53)$$

Note, that the B-phase molecules have two terminal CH_2 units, and thus two additional interring σ bonds, and R_o = 1.5 Å.

Straightforward differentiation yields

$$\frac{\partial V_\sigma^\sigma}{\partial q_L} = K_\sigma \sum_{\text{intraring}\,\sigma} (R_\sigma - R_o) \frac{\partial R_\sigma}{\partial q_L} + K'_\sigma \sum_{\text{interring}\,\sigma} (R_\sigma - R_o) \frac{\partial R_\sigma}{\partial q_L} \ . \qquad (54)$$

Summation over *L* yields for chains with a uniform *q* at all rings and also for the terminal CH_2 groups in B phase:

$$\frac{\partial V_\sigma^\sigma}{\partial q} = K_\sigma P + K'_\sigma Q$$

$$P = \sum_L \sum_{\text{intraring}\,\sigma} (R_\sigma - R_o) \frac{\partial R_\sigma}{\partial q_L}$$

$$Q = \sum_L \sum_{\text{interring}\,\sigma} (R_\sigma - R_o) \frac{\partial R_\sigma}{\partial q_L} \ . \qquad (55)$$

Thus we have the following two equations from the minimum conditions for A- and B-phase chains:

$$K_\sigma P^A + K'_\sigma Q^A + \frac{\partial E_\pi^A}{\partial q} = 0 \qquad (56a)$$

$$K_\sigma P^B + K'_\sigma Q^B + \frac{\partial E_\pi^B}{\partial q} = 0\,. \qquad (56b)$$

The solution is rather simple. Forming $(56a) \times Q^B - (56b) \times Q^A$ yields

$$K_\sigma (P^A Q^B - P^B Q^A) + \frac{\partial E_\pi^A}{\partial q} Q^B - \frac{\partial E_\pi^B}{\partial q} Q^A = 0 \qquad (57)$$

and thus

$$K_\sigma = \frac{\dfrac{\partial E_\pi^B}{\partial q} Q^A - \dfrac{\partial E_\pi^A}{\partial q} Q^B}{P^A Q^B - P^B Q^A}$$

$$K'_\sigma = -\frac{1}{Q^A}\left(K_\sigma P^A + \frac{\partial E_\pi^A}{\partial q}\right). \qquad (58)$$

In Table VI we list again the potential constants and aromatization energies for chains of lengths between 2 and 200. In the Table also the total energies of the two phases are included. The Φ-potential is the same as in models A and B. Minima in A and B for q and Φ have been checked in all cases by explicit calculation of the respective systems, shifted by ±0.001 Å and ±0.1°, respectively, from equilibrium. Note that from $N = 160$ the shifts had to be changed to ±0.0001 Å and ±0.01°, respectively, because the errors in the numerical gradients became too large. The aromatization energy is calculated again as

$$E_{A-B} = \frac{1}{N}[E_A - (E_B + 2I_C + 2\beta_{C=C}(P_{i_1,j_1} + P_{i_2,j_2}) - \\ -K'_\sigma (R_{C=C} - R_o)^2 - 2V_\phi)] \qquad (59)$$

$$\beta_{C=C} = -\beta_o e^{-\alpha_o (R_{C=C} - R^=)}; \quad \beta_o = 2.44\,\text{eV}; \quad \alpha_o = 2.91\,\text{Å}^{-1}$$

$$R^= = 1.400\ \text{Å}; \quad R_{C=C} = 1.359400\ \text{Å for biphenyl}$$

$$R_{C=C} = 1.363489\ \text{Å for all others } (N > 2); \quad R_o = 1.5\ \text{Å}$$

$$i_1 = 6; \quad j_1 = 6N + 1; \quad i_2 = 6(N - 1) + 3; \quad j_2 = 6N + 2$$

where as before I_C = 11.54 eV is the ionization potential of carbon and N the number of rings in the chain. In this way again energy contributions in E_B, resulting from the terminal CH_2 groups, should be removed as well as possible.

The Table shows clearly that now all the potential constants converge rather nicely with N, also the total energies are now all negative and decreasing with increasing N. K_σ seems to be somewhat large, but keep in mind that K_σ includes still two sets of symmetrically different intraring σ-bonds. One set includes the four bonds which bind to the bridge carbon atoms in the ring, while the other set contains the two bonds that do not connect to the bridges. However, having only two minimum structures, A and B, only two potential constants can be determined. Strangely, the

TABLE VI

The potential constants K_σ, K'_σ, and V_Φ, together with the total energies of the corresponding chains in A and B phases and the aromatization energies $E_{A–B}$ (see text for details), for increasing number of rings N, calculated with potential model C and with two terminal CH_2 groups at each B-phase chain

N	K_σ, eV/Å^2	K'_σ, eV/Å^2	V_Φ, eV	E_A, eV	E_B, eV	$E_{A–B}$ meV/ring
2	94.75	90.42	0.865	–171.59	–196.74	–2187.93
3	101.65	87.51	0.951	–256.51	–281.22	–1520.51
5	105.59	77.57	0.993	–426.65	–451.10	–970.12
10	105.50	62.23	1.016	–853.02	–877.50	–498.70
20	103.45	51.60	1.025	–1707.05	–1731.93	–237.87
40	101.83	45.82	1.030	–3415.87	–3441.48	–103.25
60	101.12	43.68	1.031	–5125.00	–5151.33	–57.43
80	100.73	42.56	1.032	–6834.23	–6861.28	–34.30
100	100.48	41.87	1.032	–8543.50	–8574.28	–20.34
120	100.31	41.41	1.033	–10252.80	–10281.30	–11.01
140	100.18	41.07	1.033	–11962.11	–11991.33	–4.33
150	100.13	40.94	1.033	–12816.76	–12846.34	–1.65
160	100.09	40.82	1.033	–13671.42	–13701.36	+0.69
180	100.01	40.62	1.033	–15380.75	–15411.41	+4.60
200	99.95	40.46	1.033	–17090.07	–17121.45	+7.73

aromatization energy still turns into a positive, increasing number from N = 160. But note that this does not mean that also in ionic systems the quinoid structure is favored over the aromatic one. We will see below in the optimizations that this is actually not the case.

For the sake of completeness, Table VII shows the corresponding set of values for the case of a B phase without having terminal CH_2 groups, not even in the determination process of the potential constants.

Note, however, that the set is somewhat unrealistic, because now every B-phase chain is conjugated throughout, with an unsaturated carbon (three single bonds only) at each end of the chain. Also here, minima in A and B for q and Φ have been checked in all cases by explicit calculation of the respective systems shifted by ±0.0001 Å and ±0.01°, respectively, from their

TABLE VII
The potential constants K_σ, K'_σ, and V_Φ, together with the total energies of the corresponding chains in A and B phases and the aromatization energies $E_{A–B}$ (here just $E_A - E_B$), for increasing number of rings N, calculated with potential model C, without two terminal CH_2 groups at each B-phase chain

N	K_σ, eV/Å^2	K'_σ, eV/Å^2	V_Φ, eV	E_A, eV	E_B, eV	$E_{A–B}$ meV/ring
2	85.44	–83.12	0.865	–172.19	–172.24	+27.39
3	83.83	–21.28	0.951	–258.27	–258.36	+28.52
5	87.06	+6.98	0.993	–429.68	–429.84	+31.72
10	91.84	+24.09	1.016	–857.44	–857.78	+33.93
20	95.19	+31.75	1.025	–1712.36	–1713.06	+34.99
40	97.17	+35.41	1.030	–3421.84	–3423.26	+35.52
60	97.88	+36.61	1.031	–5131.23	–5133.37	+35.70
80	98.24	+37.21	1.032	–6840.60	–6843.46	+35.79
100	98.46	+37.56	1.032	–8549.95	–8553.54	+35.84
120	98.61	+37.80	1.033	–10259.31	–10263.61	+35.88
140	98.72	+37.97	1.033	–11968.65	–11973.68	+35.90
160	98.80	+38.10	1.033	–13678.00	–13683.75	+35.92
180	98.86	+38.19	1.033	–15387.35	–15393.82	+35.94
200	98.92	+38.27	1.033	–17096.69	–17103.88	+35.95

equilibrium geometries. Obviously, also here all the values converge with increasing N and all total energies are negative and minima. The aromatization energy in this case is positive for all N, and thus the quinoid form is for all neutral chains more stable than the aromatic one. However, this form should not be used because for the lower members, N = 2 and 3, one of the force constants is even negative, what is non-physical for a force constant.

Therefore in all the following calculations in Section III we use potential model C including terminal CH_2 groups in the B form. Now we want to turn briefly to a very artificial way to fix the minima such that the aromatic one is the more stable one also in the neutral chains.

II.3.4. An Artificial Potential to Fix the Aromatization Energy

For that purpose, assume an asymmetric potential function $V(x)$ of some arbitrary coordinate x in arbitrary units:

$$V(x) = \frac{1}{4}x^4 + \frac{1}{3}Bx^3 + \frac{1}{2}Cx^2 \qquad (60)$$

where B and C are some, so far arbitrary, constants. Then the first two derivatives are

$$V'(x) = x^3 + Bx^2 + Cx$$

$$V''(x) = 3x^2 + 2Bx + C\,. \qquad (61)$$

Thus the condition for extrema x_i is $V'(x_i) = 0$ which is fulfilled for $x_1 = 0$. Since $V''(0) = C$, the requirement $C < 0$ makes x_1 to a maximum. Dividing $V'(x)$ by $(x - x_1) = x$ yields the equation for the other two extrema:

$$x^2 + Bx + C = 0 \Rightarrow$$

$$\Rightarrow x^2 + Bx + \frac{B^2}{4} = \frac{B^2}{4} - C \Rightarrow$$

$$\Rightarrow x_{2;3} = -\frac{B}{2}\left(1 \pm \sqrt{1 - \frac{4C}{B^2}}\right). \qquad (62)$$

To ask for minima in $x_{2;3}$, one has to ensure that

$$\frac{3}{4}B^2\left(1\pm\sqrt{1-\frac{4C}{B^2}}\right)^2 - B\left(1\pm\sqrt{1-\frac{4C}{B^2}}\right)+C>0\,. \qquad (63)$$

Note that generally $V(x_2) < V(x_3)$ where x_2 is the negative, x_3 the positive extremum. In the case of a symmetric potential function ($B = 0$) the two would be equal.

The question arises now how x has to be modified to yield q and a lower minimum at $q = +1$ (aromatic). A comparison of the geometry *Ansätze* in q and x

$$\boldsymbol{R} = \boldsymbol{R}_{\mathrm{A}} + \frac{1}{2}(1-q)(\boldsymbol{R}_{\mathrm{B}} - \boldsymbol{R}_{\mathrm{A}})$$

$$\boldsymbol{R} = \boldsymbol{R}_{\mathrm{A}} + \frac{x_2 - x}{x_2 - x_3}(\boldsymbol{R}_{\mathrm{B}} - \boldsymbol{R}_{\mathrm{A}}) \qquad (64)$$

yields directly the answer:

$$\frac{1}{2}(1-q) = \frac{x_2 - x}{x_2 - x_3} \qquad (65)$$

or

$$x = x_2 - \frac{1}{2}(1-q)(x_2 - x_3)$$

$$q = 1 - 2\frac{x_2 - x}{x_2 - x_3}\,. \qquad (66)$$

Note that the addition of such a potential function, $V(q)$, to the total potential of the system changes nothing in the predetermined positions of the minima, but could force the A phase to become the more stable one. However, without an *ab initio* determination of the energy difference between A and B phases, the use of such a potential with two parameters, B and C, which can be freely chosen, would introduce a far too large degree of arbitrariness into the model. Further, at the moment we are not in a position to perform polymer calculations on the optimized aromatic and quinoid structures of the polymer. However, the potential which would have to be added to the total energy would be

$$V = \sum_{J=1}^{N} \left[\frac{1}{4} x_J^4 + \frac{1}{3} B x_J^3 + \frac{1}{2} C x_J^2 \right]$$

$$x_J = x_2 - \frac{1}{2}(1 - q_J)(x_2 - x_3)$$

$$x_2 = -\frac{B}{2}\left(1 + \sqrt{1 - \frac{4C}{B^2}}\right); \quad x_3 = -\frac{B}{2}\left(1 - \sqrt{1 - \frac{4C}{B^2}}\right). \qquad (67)$$

This potential would leave the positions of the minima unchanged, but the maximum positions (not determined so far) would for sure not be at $q = 0$, which was anyway not expected. An example for $V(x)$ is the case $B = 0.5$ and $C = -1$. In this example $x_2 = -1.28$ and $x_3 = 0.78$, leading to the maximum position at $q = -0.24$. In a previous paper[38] we reported that the energy difference between A and B phases in *cis*-polyacetylene converges to about –7 meV/CH, when extrapolated to MP4 results. Kievelson, Su, Schrieffer, and Heeger[4] stated that the corresponding energy difference should be approximately of the same order of magnitude in ring compounds. Thus we should expect about –30 to –50 meV/ring in poly(*p*-phenylene). This could be introduced simply by adding the above discussed potential to the total energy, using the parameters $B = 0.12$ eV/Å^3 and $C = -1$ eV/Å^2, and 1/4 eV/Å^4 at the quartic term leading to an appropriate potential (in eV). Note that in Eq. (*67*) in this case x_J, x_2 and x_3 are in Å (important in the equations defining x_2 and x_3), while instead of $(1 - q_J)$ one has to write $(1 - q_J/\text{Å})$. With those parameters, the minima are $x_2 = -1.062$ Å and $x_3 = 0.941$ Å, with the maximum at $q = -0.599$ Å. The minima are at –0.294 and –0.213 eV corresponding to an energy difference of –80.4 meV between A and B phases. Figure 5 shows this type of potential.

Equation (*67*) has to be rewritten to

$$V = \sum_{J=1}^{N} \left[\frac{1}{4} \frac{\text{eV}}{\text{Å}^4} x_J^4 + \frac{1}{3} B x_J^3 + \frac{1}{2} C x_J^2 \right]$$

$$x_J = x_2 - \frac{1}{2}\left(1 - \frac{q_J}{\text{Å}}\right)(x_2 - x_3)$$

$$x_2 = -\frac{B}{2}\frac{\text{Å}^4}{\text{eV}}\left(1 + \sqrt{1 - \frac{4C}{B^2}\frac{\text{eV}}{\text{Å}^4}}\right); \quad x_3 = -\frac{B}{2}\frac{\text{Å}^4}{\text{eV}}\left(1 - \sqrt{1 - \frac{4C}{B^2}\frac{\text{eV}}{\text{Å}^4}}\right). \qquad (68)$$

III. BIPOLARON STRUCTURE OPTIMIZATIONS

To this end, we calculated chains of different lengths with a bipolaron structure on them. For the potential, model C and the constants optimized using saturating terminal CH_2 groups in the B-phase chains were used. The bipolaron geometry is

$$\frac{q_I}{\text{Å}} = 1 + \tanh[\kappa(L - I)] + \tanh[\kappa(L + I - N - 1)]\,. \qquad (69)$$

The change from A to B phase in this geometry occurs at site L and the change from B back to A phase at $N - L + 1$. The width of that change is termed κ. The angle Φ is interpolated in a linear fashion between Φ^{A}_{o} for A phase and 0 for B phase. Further it is assumed that the mean value of the aromatization coordinates of rings $I - 1$ and I determine the angle by which ring I is rotated against ring $I - 1$:

$$\phi_I = \phi_{I-1} + \frac{1}{2}\left[1 + \frac{q_I + q_{I-1}}{2\ \text{Å}}\right]\phi^{A}_{o}\ . \qquad (70)$$

Table VIII shows the results of calculations on chains with 100 and 200 rings having different values of the width of the A–B change.

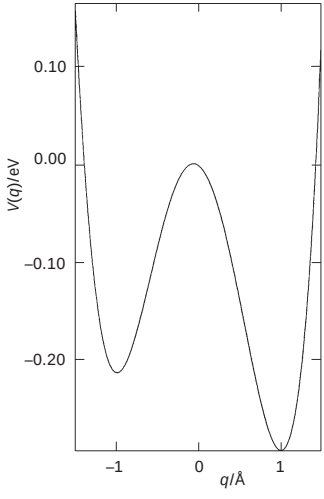

FIG. 5
An artificial potential function $V(q)$ (in eV), where q (in Å) is the collective aromatization coordinate with B = 0.12 eV/Å^3 and C = –1 eV/Å^2 to fix minima and aromatization energy (see II.3.4. for details)

The Table gives the position and energy of the largest maximum near to the chain end, as well as that of the lower one in the center of the chain. Near to the center of the chain appears a minimum at L = 48 and 98, respectively. For both chain lengths the energy minimum occurs there when κ^{-1} is around 2.0. In some cases of low κ^{-1} values there are some oscillations of the energy when L comes close to the chain end. The Table shows clearly that the very small bipolaron width is converged both for the chain with 100, as well as for that with the 200 rings.

In Fig. 6 we show a plot of the energy difference between the chains having their A–B changes at L and that one which has the total maximum energy as function of L for a chain of 100 rings and κ^{-1} = 2.0.

Figure 6 shows the complete curve, for all L from L = 1 to L = 50. Obviously there is a shallow minimum close to the center of the chain, for which L is the minimum position of the A–B change for a very small bipolaron, actually far smaller than expected. The energy increases rather

TABLE VIII

Energies per ring of the first and second maximum and of the bipolaron minimum in a chain with two positive charges and a bipolaron structure in it, where the geometry goes from aromatic over to quinoid in site L, and from quinoid back to aromatic in site $N - L + 1$. Site L is changed in each calculation from L = 1 to $L = N/2$, where N is the chain length. Note that in most cases some oscillations occur when L is approaching the chain end

N	κ^{-1}	$L_{max,1}$	$E_{max,1}$, eV/ring	$L_{min,1}$	$E_{min,1}$, eV/ring	$L_{max,2}$	$E_{max,2}$, eV/ring
100	0.5	8	–85.360001	48	–85.407326	50	–85.405527
100	1.0	9	–85.361506	48	–85.407382	50	–85.405483
100	1.5	10	–85.363047	48	–85.407422	50	–85.405362
100	2.0	10	–85.364480	48	–85.407439	50	–85.405220
100	4.0	14	–85.369898	48	–85.407271	50	–85.404793
100	6.0	16	–85.374790	48	–85.406870	50	–85.404554
200	0.1	7	–85.380862	98	–85.436490	100	–85.435560
200	1.1	9	–85.382596	98	–85.436528	100	–85.435572
200	2.1	11	–85.384395	98	–85.436551	100	–85.435437
200	4.0	15	–85.387454	98	–85.436466	100	–85.435237
200	6.0	18	–85.390532	97	–85.436292	100	–85.435118
200	8.0	22	–85.393269	97	–85.436187	100	–85.435045

steeply when L moves towards the chain end, goes through a maximum around L = 10 and then falls again steeply. A deep minimum is reached at L = 2, while at L = 1 the energy rises again a little bit.

To illustrate the reason for that unexpectedly small bipolaron width, we give in Table IX for the minimum position L = 48 in a 100-ring chain, the displacement coordinates q_K for each ring and the positive charge on each ring between ring numbers 40 and 61.

If we count the bipolaron width until q reaches 0.76 Å, then the width of the structure is obviously about 10 rings. However, it is so compressed that the fully quinoid structure is not even developed, but the lowest value of q is just –0.67 Å. The remarkable effect is that obviously no charge separation at all takes place, but only a uniform delocalization, while we would have expected that one charge would be localized at one of the bipolaron borders and the other one at the other border. In this way the driving force for a larger bipolaron width is completely missing from the system: the repulsion between the two localized like charges. The only driving force remaining is the one originating from the unfavorable B-phase segment. This force, however, tends to reduce the width of the bipolaron, as it is observed.

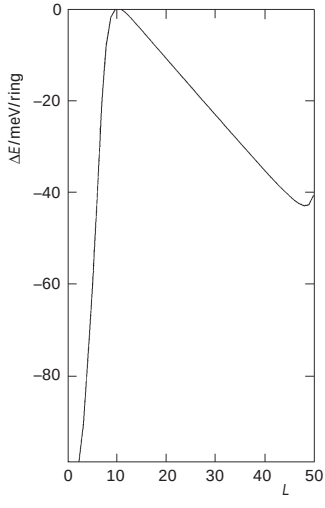

FIG. 6

Plot of the energy difference between a doubly charged (two positive charges) chain of 100 rings with a bipolaron structure in it, starting at a site L and that one with the maximum energy per ring. The reciprocal width of the aromatic-to-quinoid change is κ^{-1} = 2.0, and the site L, where the change is centered, is moving from the chain end to its center (complete curve)

Table X gives the displacement coordinates q_K and the charges, Q_K, on each ring K for chains with L values of 1, 2, 5, 10, and 15.

From the maximum $L = 10$ moving with the bipolaron towards the center of the chain and towards decreasing width of the bipolaron, the energy decreases, probably because the size of the B-phase segment decreases in the same direction. Thus in contrast to many neutral chain cases, in the charged ones clearly the aromatic A phase is favored over the quinoid B phase. At the maximum, $L = 10$, the change in geometry starts to affect the chain end, unit no. 1, in this way forming an increasingly quinoid, and thus increasingly unsaturated, end ring. However, coincidentally, the positive charge at the end ring also increases, increasing the saturation. This is the reason why the energy decreases again when going with L from the maximum, $L = 10$, closer to the chain end. However, when L is equal to the chain end, the charge becomes somewhat compressed and therefore the energy rises again a little when L reaches 1, creating a minimum at $L = 2$.

TABLE IX

The displacement coordinates q_K for each ring K and the charges Q_K (in units of the elementary charge e = 1.602×10^{-19} As) on each ring K in a chain of 100 rings with a minimum energy doubly positive bipolaron structure ($L = 48$) in its center for $\kappa^{-1} = 2.0$ between rings #40 and #61

K	q_K, Å	Q_K, e	K	q_K, Å	Q_K, e
40	1.00	0.00	51	–0.67	0.41
41	1.00	0.00	52	–0.43	0.31
42	1.00	0.00	53	0.00	0.18
43	0.99	0.00	54	0.47	0.07
44	0.96	0.00	55	0.76	0.02
45	0.91	0.01	56	0.91	0.01
46	0.76	0.02	57	0.96	0.00
47	0.47	0.07	58	0.99	0.00
48	0.00	0.18	59	1.00	0.00
49	–0.43	0.31	60	1.00	0.00
50	–0.67	0.41	61	1.00	0.00

TABLE X

The displacement coordinates q_K for each ring K and the charges Q_K (in units of the elementary charge $e = 1.602 \times 10^{-19}$ C) on each ring K in chains of 100 rings with a doubly positive bipolaron structure in their centers for $\kappa^{-1} = 2.0$ with the aromatic-to-quinoid change in sites $L = 1$, 2, 5, 10, and 15, shown between rings No. 1 and 10 for the first three and 6 and 20 for the last two

	$L = 1$ $E_1 = -85.4621$ eV/ring		$L = 2$ $E_2 = -85.4634$ eV/ring		$L = 5$ $E_5 = -85.4242$ eV/ring	
K	q_K, Å	Q_K, e	q_K, Å	Q_K, e	q_K, Å	Q_K, e
1	0.00	0.0001	0.46	0.0000	0.96	0.0000
2	–0.46	0.0002	0.00	0.0002	0.91	0.0000
3	–0.76	0.0005	–0.46	0.0003	0.76	0.0000
4	–0.91	0.0007	–0.76	0.0006	0.46	0.0001
5	–0.96	0.0011	–0.91	0.0009	0.00	0.0002
6	–0.99	0.0015	–0.96	0.0013	–0.46	0.0004
7	–1.00	0.0020	–0.99	0.0018	–0.76	0.0006
8	–1.00	0.0026	–1.00	0.0023	–0.91	0.0010
9	–1.00	0.0032	–1.00	0.0029	–0.96	0.0015
10	–1.00	0.0039	–1.00	0.0036	–0.99	0.0021

	$L = 10$ $E_{10} = -85.3645$ eV/ring		$L = 15$ $E_{15} = -85.3688$ eV/ring	
K	q_K, Å	Q_K, e	q_K, Å	Q_K, e
6	0.96	0.0000	1.00	0.0000
7	0.91	0.0000	1.00	0.0000
8	0.76	0.0000	1.00	0.0000
9	0.46	0.0001	1.00	0.0000
10	0.00	0.0002	0.99	0.0000
11	–0.46	0.0004	0.96	0.0000
12	–0.76	0.0008	0.91	0.0000
13	–0.91	0.0013	0.76	0.0000
14	–0.96	0.0020	0.46	0.0001
15	–0.99	0.0027	0.00	0.0003
16	–1.00	0.0036	–0.46	0.0006
17	–1.00	0.0046	–0.76	0.0012
18	–1.00	0.0057	–0.91	0.0019
19	–1.00	0.0069	–0.96	0.0029
20	–1.00	0.0082	–0.99	0.0040

IV. CONCLUSION

Obviously, the use of the Hückel-type picture has two shortcomings for the description of bipolarons. The first one is that, unexpectedly for larger chains, the aromatic phase becomes less favorable than the quinoid one for neutral chains, which is not the case for charged ones. In accordance with Paldus' notion of the importance of explicit electron electron interactions, we hope that this shortcoming might be cured, when in the future we use a Pariser–Parr–Pople hamiltonian. However, even if this would not be case, the existence of a fully conjugated system of double bonds in a quinoid chain might account for this unexpected behavior.

More crucial is the fact that the expected separation of the two charges does not occur, creating an extremely small bipolaron. In a PPP description, maybe even a correlated or DFT type model might be needed. Then the frontier orbital, from which the two electrons are removed in order to create the two positive charges, might be more sensitive to the disorder around the sites where the A–B changes occur, showing maxima of its density there, and thus separating charges on those rings. Actually this had been already discussed in the literature[41] on the basis of a Hubbard-type hamiltonian

However, for this a spin separation could be necessary either. So one maybe would have to use an unrestricted PPP (UPPP) type of model, which can have a single maximum in the orbital of one of the two spins at one phase change, and another single maximum in the orbital of the other spin at the other phase change. If it turns out that spin separation is necessary either, simple UPPP cannot be used because of the appearance of spin contaminations there, making UPPP geometry predictions extremely unreliable (Paldus et al.[42]). Then one has to use an annihilated UPPP method[43], as we used in calculations on open-shell polyacetylene chains. The seemingly better extended PPP method could not be used because, as shown by Martino and Ladik[44], the extended method converges back to the unrestricted one with increasing system size. The RPPP (restricted closed-shell PPP), the UPPP and the AUPPP methods are currently under programming (the debugging process is not yet completed) and the results will be the subject of a forthcoming publication.

The author wants to thank King Fahd University of Petroleum and Minerals for funding the present research via project CY/NONLINEAR/216. Further the author wants to thank Dr. H. M. Badawi for the possibility to use his IBM workstation and for his invaluable help in some of the calculations reported here.

REFERENCES

1. Su W. P., Schrieffer J. R., Heeger A. J.: *Phys. Rev. Lett.* **1979**, *42*, 1698.
2. Su W. P.: *Solid State Commun.* **1980**, *35*, 899.
3. Su W. P., Schrieffer J. R., Heeger A. J.: *Phys. Rev. B* **1980**, *22*, 2099.
4. Heeger A. J., Kivelson S., Schrieffer J. R., Su W. P.: *Rev. Mod. Phys.* **1988**, *60*, 781.
5. Su W. P., Schrieffer J. R.: *Proc. Natl. Acad. Sci. U.S.A.* **1980**, *77*, 5626.
6. Liegener C.-M., Förner W., Ladik J.: *Solid State Commun.* **1987**, *61*, 203.
7. Baeriswyl D.: *Synth. Met.* **1993**, *55–57*, 4231.
8. a) Pariser R., Parr R. G.: *J. Chem. Phys.* **1953**, *21*, 660; b) Pariser R., Parr R. G.: *J. Chem. Phys.* **1953**, *21*, 707.
9. Pople J. A.: *Trans. Faraday Soc.* **1953**, *49*, 1375.
10. Ladik J.: *Acta Phys. Acad. Sci. Hung.* **1965**, *18*, 185.
11. Ladik J., Rai D. K., Appel K.: *J. Mol. Spectrosc.* **1968**, *27*, 72.
12. Ladik J.: *Quantenchemie*. F. Enke Verlag, Stuttgart 1973.
13. Förner W.: *Phys. Rev. B* **1991**, *44*, 11743.
14. Förner W.: *Adv. Quantum Chem.* **1994**, *25*, 207.
15. Boudreaux D. S., Chance R. R., Bredas J. L., Silbey R.: *Phys. Rev. B* **1983**, *28*, 6927.
16. Enim D.: *Phys. Rev. B: Condens. Matter* **1986**, *33*, 3973.
17. Garstein Y. N., Zakhidov A. A.: *Solid State Commun.* **1986**, *60*, 105.
18. Vogl P., Campbell D. K.: *Phys. Rev. B* **1990**, *41*, 12797.
19. Conwell E. M., Mizes H. A.: *Synth. Met.* **1993**, *55–57*, 4284.
20. Blackman J. A., Sabra M. K.: *Phys. Rev. B* **1993**, *47*, 15437.
21. Rothberg L., Jedju T. M., Townsend P. D., Etemad S., Baker G. L.: *Phys. Rev. Lett.* **1990**, *65*, 100.
22. Sinclair M., Moses D., Heeger A. J.: *Solid State Commun.* **1986**, *59*, 343.
23. Boman M., Stafström S.: *Synth. Met.* **1993**, *55–57*, 4614.
24. Su W. P.: *Solid State Commun.* **1982**, *42*, 497.
25. Nakahara M., Maki K.: *Phys. Rev. B* **1982**, *25*, 7789.
26. Hirsch J. E., Sugar R. L., Scalapino D. J., Blankenbeckler R.: *Phys. Rev. B* **1982**, *26*, 5033.
27. a) Hirsch J. E., Fradkin E.: *Phys. Rev. B: Condens. Matter* **1983**, *27*, 1680; b) Hirsch J. E., Fradkin E.: *Phys. Rev. B* **1983**, *27*, 4302.
28. Nakahara M., Maki K.: *Synth. Met.* **1986**, *13*, 149.
29. Sum U., Fesser K., Büttner H.: *Phys. Rev. B* **1989**, *40* 10509.
30. Wang C. L., Su Z. B., Martino F.: *Phys. Rev. B* **1986**, *33*, 1512.
31. Bredas J. L., Chance R. R., Silbey R.: *Mol. Cryst. Liq. Cryst. Sci. Technol., Sect. A* **1981**, *77*, 319.
32. Bredas J. L., Chance R. R., Silbey R.: *Phys. Rev. B* **1981**, *26*, 5843.
33. Bredas J. L., Themans B., Fripiat J. G., Andre J. M., Chance R. R.: *Phys. Rev. B* **1984**, *29*, 6761.
34. Epstein A. J.: *Handbook of Conducting Polymers*, Vol. 2, p. 1041. Dekker, New York, Basel 1986.
35. Förner W., Utz W.: *J. Mol. Struct. (THEOCHEM)* **2002**, *618*, 65.
36. Förner W.: *J. Mol. Struct. (THEOCHEM)* **2004**, *682*, 115.
37. a) Förner W.: *Chem. Phys.* **1992**, *160*, 173; b) Förner W.: *Chem. Phys.* **1992**, *160*, 189.
38. Utz W., Förner W.: *Phys. Rev. B* **1998**, *57*, 10512.
39. Förner W.: *Solid State Commun.* **1987**, *63*, 941.

40. Frisch M. J., Trucks G. W., Schlegel H. B., Scuseria G. E., Robb M. A., Cheeseman J. R., Zakrzewski V. G., Montgomery J. A., Jr., Stratmann R. E., Burant J. C., Dapprich S., Millam J. M., Daniels A. D., Kudin K. N., Strain M. C., Farkas O., Tomasi J., Barone V., Cossi M., Cammi R., Mennucci B., Pomelli C., Adamo C., Clifford S., Ochterski J., Petersson G. A., Ayala P. Y., Cui Q., Morokuma K., Malick D. K., Rabuck A. D., Raghavachari K., Foresman J. B., Cioslowski J., Ortiz J. V., Baboul A. G., Stefanov B. B., Liu G., Liashenko A., Piskorz P., Komaromi I., Gomperts R., Martin R. L., Fox D. J., Keith T., Al-Laham M. A., Peng C. Y., Nanayakkara A., Gonzalez C., Challacombe M., Gill P. M. W., Johnson B., Chen W., Wong M. W., Andres J. L., Gonzalez C., Head-Gordon M., Replogle E. S., Pople J. A.: *Gaussian 98*, Revision A.7. Gaussian, Inc., Pittsburgh (PA) 1998.
41. Alexandrov A. S., Kornilovitch P. E.: *J. Phys.: Condens. Matter* **2002**, *14*, 5337; and references therein.
42. a) Paldus J., Chin E.: *Int. J. Quantum Chem.* **1983**, *24*, 373; b) Paldus J., Chin E., Grey M. G.: *Int. J. Quantum Chem.* **1983**, *24*, 395.
43. Kovar T.: *MS Thesis*. Friedrich-Alexander University, Erlangen-Nürnberg 1986.
44. Martino F., Ladik J.: *Phys. Rev. A* **1971**, *3*, 862.